**NURETH14-530** 

# NUMERICAL PREDICTION ON SUBCOOLED BOILING BUBBLE BEHAVIOR

Y. Ose<sup>1</sup> and T. Kunugi<sup>1</sup>
<sup>1</sup> Kyoto University, Kyoto, Japan

#### **Abstract**

This study focuses on the subcooled pool boiling. Since the subcooled pool boiling is occurred under a condition below the saturation temperature, it is the most complex phenomenon consisted of the bubble growth, condensation and extinction processes with phase-change phenomena: evaporation and condensation. Although the subcooled boiling is very important phenomena, the essential mechanism has not yet been clarified until now because the bubble nucleation and growth processes are too fast to observe even by means of a very high-speed camera. Another approach to understand these processes is a numerical simulation. In this study, in order to clarify the heat transfer characteristics of the subcooled pool boiling and to discuss its mechanism, a boiling and condensation model for numerical simulation on subcooled boiling phenomena has been developed. In this paper, the three dimensional numerical simulations based on the MARS (Multi-interface Advection and Reconstruction Solver) with the boiling and condensation model consisted of the improved phase-change model and an introduction of the relaxation time based on the quasi-thermal equilibrium state have been conducted for the subcooled pool boiling phenomena especially regarding to the bubble departure behavior from the heated surface. The results of the numerical simulations were compared with the experimental data obtained by the high-speed camera (Phantom 7.1) with the Cassegrain optical system, and then the influence of the degree of subcooling for the bubble departure and the heat transfer on the heated surface were numerically predicted. As the results, the numerical results of bubble departure behavior from the heated surface showed in good agreement with the experimental observations quantitatively.

## Introduction

Boiling phenomena is a key to remove the heat from the fuel rods in nuclear reactors such as BWR (Boiling Water Reactor) because the boiling heat transfer has enormous heat transfer coefficient compared to the convection of single-phase flows. It will also play a significant role of the thermal management in nuclear reactors. Therefore, in order to clarify the mechanism of boiling phenomena, it has been studied extensively over the decades.

This study focuses on the subcooled pool boiling. Since the subcooled boiling is occurred under a condition below the saturation temperature, it is the most complex phenomenon compared to the saturated boiling, because it includes not only the convective heat transfer but also the rapid evaporation and condensation processes. It is also known that the critical heat flux of the subcooled boiling is greater than that of saturated boiling. Although the subcooled boiling is very important phenomenon mentioned above, the essential mechanism has not yet

been experimentally clarified until today because the bubble nucleation and growth processes are too fast to observe even by using the current high speed camera. On the other hand, the numerical simulation is more promising as an alternative approach to understand these processes. Since the prediction of boiling phenomena is very important for the thermal designs and managements, it has been proposed numerous prediction models with some empirical correlations based on the experimental data and/or theoretical considerations. However, there is no "direct" numerical model for the subcooled boiling because of the limitation of the experimental data and the theoretical considerations: here, "direct" means "without any empirical correlation for the boiling heat transfer."

In recent years, with great advances in computer power, numerical simulations for directly treating the bubble dynamics regarding the nucleate boiling have been performed by several investigators [1-6]. However, these simulations were only performed the saturated boiling conditions, the direct numerical simulation in subcooled boiling has also hardly been reported until now.

In this study, it is focused on the clarification of the heat transfer characteristics of the subcooled pool boiling, the discussion on its mechanism, and the establishment of a boiling and condensation model for the direct numerical simulation on the subcooled pool boiling phenomena. In this paper, the boiling and condensation model has been improved by introducing the following models based on the quasi-thermal equilibrium hypothesis: (1) an improved phase-change model which consisted of the enthalpy method for the water-vapor systems, (2) a relaxation time derived by considering the unsteady heat conduction at the vapor-water interface. Then, unsteady three dimensional numerical simulations based on the MARS (Multi-interface Advection and Reconstruction Solver) [7] with the improved boiling and condensation model were performed for the bubble departing process from the heated surface. The results of the numerical simulations were compared with the experimental observations, and then the effect of the degree of subcooling on the bubble departing behavior including their shape changes from the heated surface and the wall heat flux were investigated.

#### 1. Numerical method

# 1.1 Governing equation

The governing equations of the MARS are consisted of the continuity equation for multiphase flows, the momentum equation based on a one-fluid model and the energy equation as follows:

$$\frac{\partial F_m}{\partial t} + \nabla (F_m \mathbf{u}) - F_m \nabla \mathbf{u} = 0 \tag{1}$$

$$\frac{\partial \mathbf{u}}{\partial t} + \nabla \cdot (\mathbf{u}\mathbf{u}) = \mathbf{G} - \frac{1}{\langle \rho \rangle} \nabla P - \nabla \cdot \tau + \frac{1}{\rho} \mathbf{F}_{\nu}$$
 (2)

$$\frac{\partial}{\partial t} \langle \rho C_{\nu} \rangle T + \nabla \cdot (\langle \rho C_{\nu} \rangle T \boldsymbol{u}) = \nabla \cdot (\langle \lambda \rangle \nabla T) - P(\nabla \cdot \boldsymbol{u}) + Q$$
 (3)

here, F is volume of fluid (VOF) fraction, the suffix m denotes the m-th fluid or phase, u is velocity, t is time, P is pressure, T is temperature, G is gravity,  $\tau$  is viscous shear stress,  $F_v$  is body force due to a surface tension based on the Continuum Surface Force (CSF) model [8],  $\rho$  is density,  $C_v$  is specific heat at constant volume,  $\lambda$  is thermal conductivity, Q is heat source and <> denotes an average of properties. In order to satisfy the conservation of F, the third term of the continuity equation (Eq. (1)) must be included. The second term of the right hand side of the energy equation (Eq. (3)), i.e., the Clausius-Clapeyron relation is considered as the external work done by the phase change, e.g., a bubble oscillation caused by the expansion and contraction with the bubble growth and condensation processes. The interface volume-tracking technique [7] is applied to the continuity equation in the MARS. The projection method [9] is applied to solve the momentum equation and its derived pressure Poisson equation is solved by the Bi-CGSTAB [10].

# 1.2 Boiling and condensation model

Nucleation of a boiling bubble needs to be modelled, because the nucleation process is not completely understood until today. The boiling and condensation model in the MARS for the subcooled nucleate boiling phenomena consists of both a nucleation model and a bubble growth-condensation model [11]. The homogeneous nucleation based on the kinetic theory [12] gives a uniform superheat limit of liquid and a size of the embryo of vapor bubble. A critical radius  $r_e$  of the embryo corresponding to the superheated limit  $T_{SH}$  can be calculated by Eq. (4).

$$r_{e} = \frac{2\sigma}{P_{ext}(T_{t}) \exp\{v_{t}[P_{t} - P_{ext}(T_{t})]/RT_{t}\} - P_{t}}; (T_{s} \ge T_{SH})$$
(4)

here,  $T_S$  is liquid temperature contacted to the heated surface,  $\sigma$  is surface tension,  $T_l$  is temperature of liquid,  $P_{sat}$  is pressure corresponding to saturation condition,  $P_l$  is pressure of liquid,  $v_l$  is specific volume of liquid, and R is ideal gas constant per unit mass basis. A computational cell having the liquid temperature over  $T_{SH}$  can be given a VOF fraction corresponding to the embryo volume. Although  $T_{SH}$  might be spatially varied on the heated surface according to the experiment [13],  $T_{SH}$  is assumed to be uniform on the heated surface, i.e., the nucleation site density is not considered in the present study [14].

The bubble growth-condensation model is based on the temperature-recovery method [15] which is the improved enthalpy method. This model is applied to only the interfacial cells which have the VOF fraction of both gas and liquid phases. However, the original model could not treat a large volume change in the expansion and condensation processes, because the temperature-recovery method was originally developed for the solidification/melting of metals not for the water-vapor phase-change system. In this study, a density-change between water and vapor was considered as a volume-change by a phase-change ratio  $\Delta g_{\nu}$ , as expressed as:

The 14<sup>th</sup> International Topical Meeting on Nuclear Reactor Thermalhydraulics, NURETH-14 Toronto, Ontario, Canada, September 25-30, 2011

$$\Delta g_{v} = \frac{\rho_{l} C_{pl} \Delta T}{\rho_{v} h_{tv}} \left[ = \frac{\text{Sensible heat}}{\text{Latent heat}} \right]$$
 (5)

here,  $C_p$  is specific heat at constant pressure,  $\Delta T$  is degree of superheat or subcooling  $(T_{sat}-T)$ ,  $h_{lv}$  is latent heat and the suffixes of g and l denote gas and liquid phases, respectively. Equation (5) means that the ratio of the sensible heat to the latent heat at the interfacial cell. In order to satisfy the conservation of the volume, the following constant condition must be satisfied:

$$(F_t + \Delta g_v) + (F_g - \Delta g_v) = 1 \tag{6}$$

The original bubble growth-condensation model was based on the assumptions of both a zero-thickness interface and a "rapid" change of "State 1: Water" to "State 2: Vapor" or *vice versa* based on the quasi-thermal equilibrium hypothesis. However in this model, a "very slow" change of "State 1" to "State 2" in the quasi-thermal equilibrium hypothesis was ignored. In the real system, the finite thickness of interface exists and both "very slow" and "rapid" changes simultaneously occur in the phase-change process. In order to consider a relaxation or waiting time for consuming the latent heat at the interface region in the phase-change process, the unsteady heat conduction in the interface region as the "very slow" change process is considered as follows: The relaxation time  $t_{\Delta}$  can be considered that the phase-change front passes through the computational cell width  $\Delta$ , so that  $t_{\Delta}$  can be defined by using the thermal diffusivity of medium  $\alpha$  as follows:

$$t_{\Lambda} \equiv \Delta^2 / \alpha \tag{7}$$

On the other hand, a thermal penetration length  $\delta$  for the unsteady heat conduction in a semi-infinite slab with a constant boundary temperature is approximated by the following expression:

$$\delta = \sqrt{12\alpha t} \tag{8}$$

If  $t_{\Delta}$  substitutes into Eq. (8),  $\delta = \sqrt{12\Delta}$ . As the result, an invariant relation between the thermal penetration length and the computational cell width can be obtained as follows:

$$\frac{\Delta}{\delta} = \left(\sqrt{12}\right)^{-1} \approx 0.3\tag{9}$$

Therefore, the rapid phase-changed volume during  $t_{\Delta}$  will be 70% of the computational cell, not 100%. This means the "very slow" change can be realized by this invariant constant. In this study, the relaxation time can be considered if a VOF limiter is introduced as a phase-change denominator or limiter. For example, the relaxation time for both phase fronts is assumed to be 15% at both interfaces of evaporation and condensation:

VOF limiter: 
$$0.15 \le F \le 0.85$$
 (10)

#### 2. Numerical simulation

# 2.1 Computational domain

In order to simulate the bubble departing behaviors observed by a visualization experiments in subcooled pool boiling, three dimensional numerical simulations based on the MARS with the improved boiling and condensation model were conducted for the bubble departing behaviors from the heated surface in the subcooled pool boiling. The visualization of the subcooled nucleate pool-boiling experiment under atmospheric pressure was conducted by using the ultra-high-speed video camera mounted on a long-focus microscope system [16].

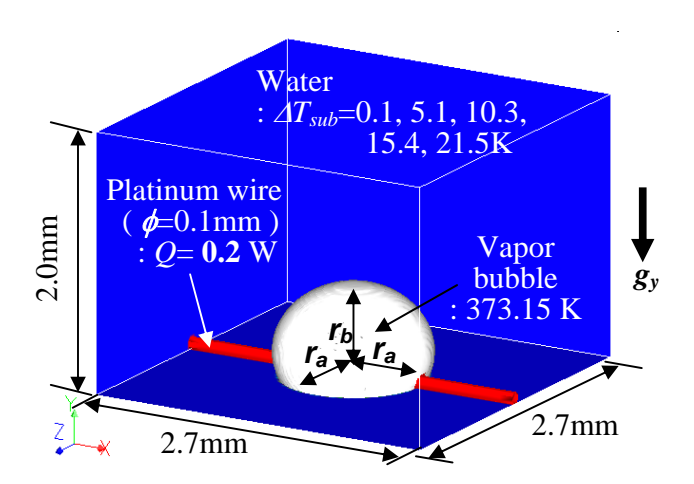


Figure 1 Computational domain.

Figure 1 shows the computational domain in this numerical simulation. The computational domain size was 2.7 mm  $\times$ 2.0 mm  $\times$ 2.7 mm. The grid size was 20–100  $\mu$ m in x- and zdirections, respectively, and was 20 µm in y- direction. The number of computational grids was 103×83×103, and time increment in the computation was set to 1µs. The periodic boundary conditions were imposed at the x- and z-directions respectively. The non-slip wall velocity boundary conditions were applied to all walls, and the upper boundary condition in ydirection was set to a constant hydraulic pressure condition. The computational conditions were basically the same as the experiments. The initial pressure was set to an atmospheric pressure and the degrees of subcooling in the water pool were set to 0.1, 5.1, 10.3, 15.4 and 21.5 K as the same as the experimental conditions. The heating platinum wire of 0.1 mm in diameter used in the experiment was located at the bottom of computational domain, and the volumetric heat source at the center of the wire was set to 0.2 W which was corresponding to the heat flux on the heated surface in the experiment: 0.25 MW/m<sup>2</sup>. The initial temperature of heating wire was set to 110°C which was estimated by using a waiting time obtained from both the experimental results and the analytical solution of unsteady heat conduction. In order to evaluate the heart transfer characteristics of the heated surface, the solid heat conduction from the center of the heating wire to its surface was numerically considered. In order to consider the wettability on the heated wire surface, the contact angle between the wire surface and the liquid was set to 20°. Since it is focused on the bubble departing behavior from the heated wire surface in this study, the initial bubble shape was assumed at the maximum bubble size in a horizontal direction obtained from the experimental data. The initial bubble diameter was thus set to as shown in Table. 1, and an initial bubble was put as a hemispherical shape at the center of the heated surface as shown in Fig. 1. The initial bubble temperature was also set to the saturated temperature corresponding to an atmospheric pressure. Although the velocity and temperature fields around the growing bubble was existed in the experiments, these initial fields in this numerical simulation was assumed to be both stationary and homogenous temperature fields with the degree of subcooling because the experimental data corresponding to these fields could not be obtained.

$\Delta T_{sub}$ [K]	$r_a$ [mm]	$r_b$ [mm]
0.1	0.70	0.51
5.1	0.62	0.47
10.3	0.56	0.48
15.4	0.49	0.38
21.5	0.44	0.35

Table 1 Table of initial bubble radius.

#### 2.2 Results and Discussions

Figures 2-(a) and -(b) show the time variation of bubble departing behavior observed in the experiments (upper) and the numerical simulation (lower) at  $\Delta T_{sub}$ =10.3 and 21.5 K, respectively. The results of numerical simulation show the bubble shapes as an iso-surface corresponding to the VOF fraction of 0.5, the temperature contours and the velocity vectors. At  $\Delta T_{sub}$ =10.3 K (Fig. 2-(a)), the numerical results retrieve the experimental one that the bubble becomes from the flattened shape in the superheated layer to the vertically-elongated one in the saturated or subcooled liquid layer before the bubble departure from the heated wire surface. At  $\Delta T_{sub}$ =21.5 K (Fig. 2-(b)), the bubble shape becomes more vertically-elongated with increase of the degree of subcooling. From the results of numerical simulation at  $\Delta T_{sub}$ =21.5 K, it is found that a large upward velocity like a jet from the bottom of bubble to the top appears when the bubble becomes the vertically-elongated shape. Figure 3 shows the comparison of bubble shapes just before the bubble departure from the heated wire surface, and also shows the comparison between experimental and numerical results at various degrees of subcooling. As a result, the bubble shapes predicted by the numerical simulations are reasonably in good agreement with those shapes obtained by the experiments.

In order to validate the time variation of bubble shape changes obtained from the numerical results, Figure 4 shows a quantitative comparison of the time variation of the bubble aspect ratio between the experimental data and the numerical simulation results at various degrees of subcooling. The open symbols depict the data corresponding to from a beginning of the bubble growth to just before the bubble departure. The solid symbols depict the data corresponding to after the bubble departure in the subcooled pool boiling. The solid line denotes the numerical results corresponding to from the beginning of the bubble growth to just before the bubble departure. As the result, the time variations of the bubble aspect ratio

obtained from the numerical results are in good agreement with the experimental data: with increase of the degree of subcooling, 1) the bubble becomes more vertically-elongated shape, 2) the time interval from the bubble nucleation to its departure from the heated surface is decreasing.

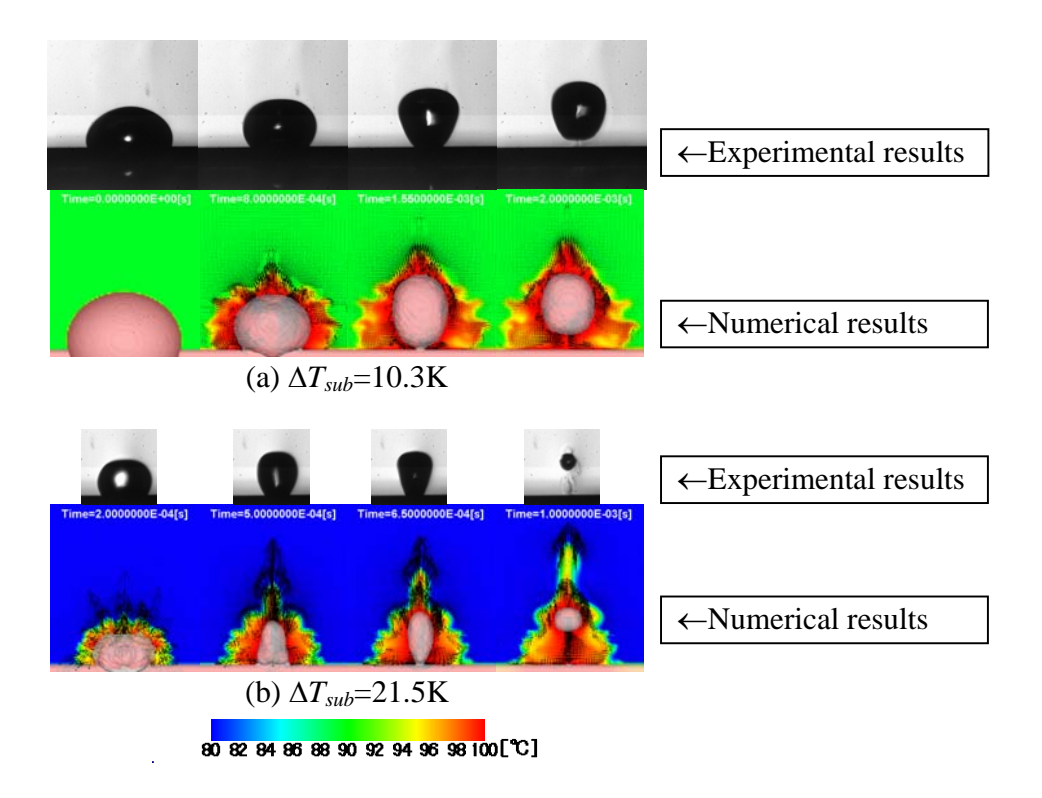


Figure 2 The comparison of the time variation of bubble departing behavior between experimental and numerical results.

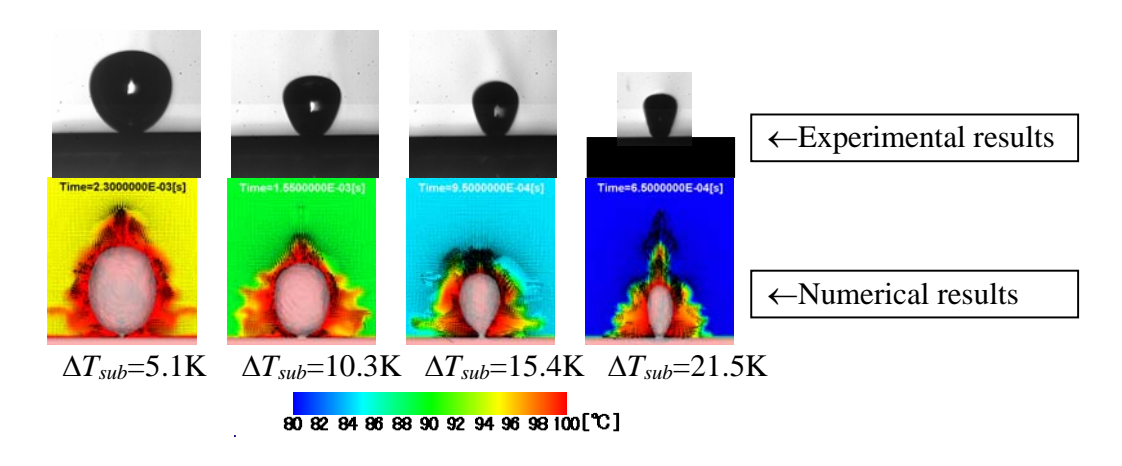


Figure 3 The comparison of bubble shapes just before bubble departing from heated surface between experimental and numerical results at various degrees of subcooling.

However, it can be seen that the numerical results are over predicted the time interval which from the bubble nucleation to its departure from the heated surface compared with the experimental data. This reason might be considered that the initial condition of numerical simulations could not be completely consistent with the experimental conditions such as the property of heated wire surface and the temperature and velocity fields around the growing bubble. Consequently, while the initial conditions both velocity and temperature fields are very important factor in order to achieve high accuracy prediction, it would say that the present numerical simulation based on the MARS with improved boiling and condensation model can predict the bubble departure from the heated surface in subcooled pool boiling behaviors as experimentally observed.

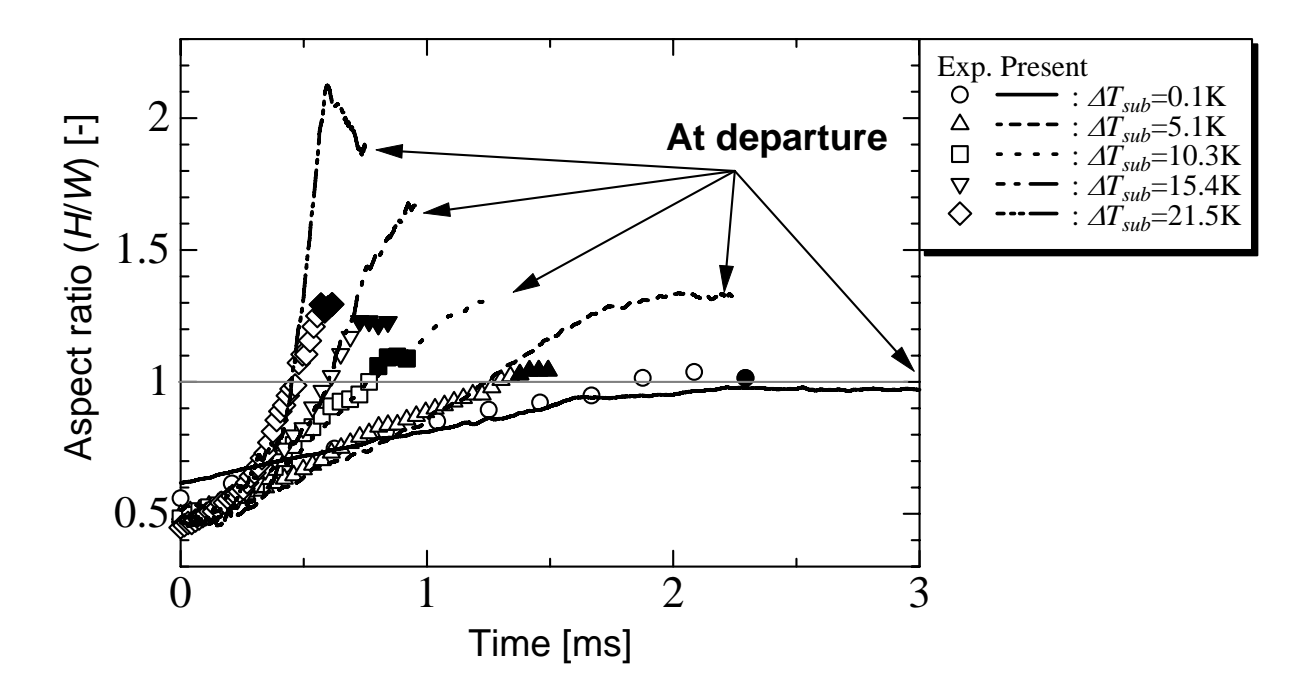


Figure 4 The comparison of time variation of bubble aspect ratio between experimental data and numerical results.

Furthermore, in order to estimate the heat transfer characteristics on the heated surface, Figure 5 shows the time variations of the wall heat flux distribution in the *x*-direction at  $\Delta T_{sub}$ =10.3K. The wall heat flux on the heated surface  $q_w$  was defined as follows,

$$q_{w} = \lambda_{f} \frac{T_{s} - T_{f}}{\Delta x}, \quad T_{s} = \frac{\lambda_{f} T_{f} \Delta x_{f} + \lambda_{w} T_{w} \Delta x_{w}}{\lambda_{f} \Delta x_{f} + \lambda_{w} \Delta x_{w}}$$
(11)

here,  $T_s$  is the heated surface temperature defined by the Eq. (11), T is temperature and  $\lambda$  is thermal conductivity.  $\Delta x$  is distance to the heated surface. The suffixes f and w denote the fluid and wall computational cells adjacent to the heated surface, respectively. As the results,

the wall heat flux is deceased from the center of the bubble at x=0 mm to the bubble interface, i.e., this region corresponds to the dry-out region, and is increased over the bubble interface to the liquid region. It is confirmed that the wall heat flux is drastically increased near the contact line at the bottom of the bubble, and it is kept until the bubble departure from the heated surface at t=1.6ms. After the bubble departure, the wall heat flux is rapidly decreased. This reason can be considered that the wall temperature is rapidly cooled by the subcooled liquid flow after the bubble departure from the heated surface because the amount of heat source in the heated wire is relatively small. These tendencies show the same results for other degree of subcooling.

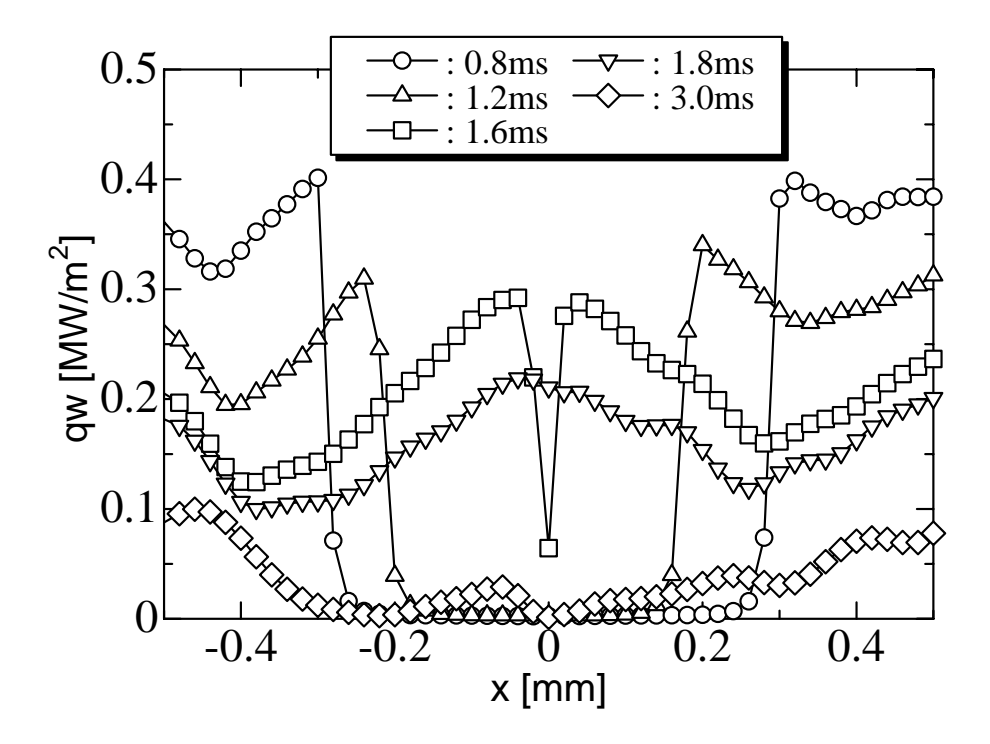


Figure 5 Wall heat flux distribution in the *x*-direction at  $\Delta T_{sub}$ =10.3 K.

Figure 6 shows the wall heat flux distribution in the *x*-direction just before the bubble departure from the heated surface at various degrees of subcooling. As the results, it is found that the wall heat flux near the contact line at the bottom of the bubble just before the bubble departing from the heated surface increases with increase of the degree of subcooling.

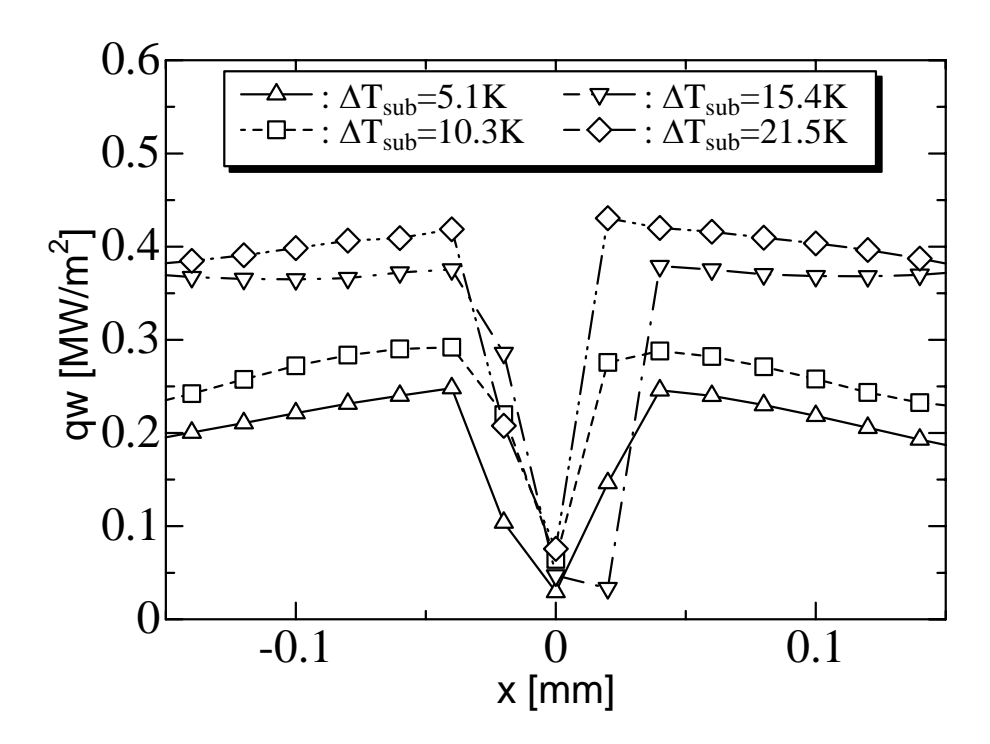


Figure 6 Wall heat flux distribution in the *x*-direction just before bubble departing from heated surface at various degrees of subcooling.

## 3. Conclusion

The numerical simulations based on the MARS with the boiling and condensation model considering the relaxation time based on the quasi-thermal equilibrium hypothesis were conducted for the bubble departing behavior from the heated wire surface in subcooled pool boiling. The results of numerical simulations were compared with the experimental results, especially for the bubble shapes. As the results, the numerical results for the bubble departing behavior showed in good agreement with the experimental results as follows:

- 1. The time interval from the bubble nucleation to its departing from the heated surface decreases with increase of the degree of subcooling.
- 2. The aspect ratio of the bubble shape increases with increase of the degree of subcooling, i.e., the bubble shape becomes more vertically-elongated before the bubble departure from the heated surface.

Furthermore, resulting from the wall heat flux evaluation, it is found that the wall heat flux near the contact line at the bottom of the bubble just before the bubble departing from the heated surface increases with increase of the degree of subcooling.

As mentioned above, it is concluded that the present boiling and condensation model can predict the bubble departing behavior from the heated surface in subcoold pool boiling.

## 4. Acknowledgments

This work was partly supported by a "Energy Science in the Age of Global Warming" of Global Center of Excellence (G-COE) program (J-051) of the Ministry of Education, Culture, Sports, Science and Technology of Japan.

### 5. References

- [1] R.C. Lee and J.E. Nydahl, "Numerical calculation of bubble growth in nucleate boiling from inception through departure", Journal of Heat Transfer, Vol. 111, No. 2, 1989, pp. 474-479.
- [2] S.W.J. Welch, "Direct simulation of bubble growth". International Journal of Heat and Mass Transfer, Vol. 41, No. 12, 1998, pp. 1655-1666.
- [3] G. Son, V.K. Dhir and N. Ramanujapu, "Dynamics and heat transfer associated with a single bubble during nucleate boiling on a horizontal surface". Journal of Heat Transfer, Vol. 121, No. 3, 1999, pp. 623-631.
- [4] H.Y. Yoon, S. Koshizuka and Y. Oka, "Direct calculation of bubble growth, departure, and rise in nucleate pool boiling". International Journal of Multiphase Flow, Vol. 27, No. 2, 2001, pp. 277-298.
- [5] S. Shin, S.I. Abdel-Khalik and D. Juric, "Direct three-dimensional numerical simulation of nucleate boiling using the level contour reconstruction method", International Journal of Multiphase Flow, Vol. 31, No. 10, 2005, pp. 1231-1242.
- [6] G. Son and V.K. Dhir, "Numerical simulation of nucleate boiling on a horizontal surface at high heat fluxes", International Journal of Heat and Mass Transfer, Vol. 51, No. 9-10, 2008, pp. 2566-2582.
- [7] T. Kunugi, "MARS for multiphase calculation", Computational Fluid Dynamics Journal, Vol. 9, No. 1, 2001, pp. 563-571.
- [8] J.U. Brackbill, D.B. Kothe and C. Zemach, "A continuum method for modeling surface tension". Journal of Computational Physics, Vol. 100, No. 2, 1992, pp. 335-354.
- [9] A. Chorin, "Numerical solution of the navier-stokes equations". Mathematics of Computation, Vol. 22, No.104, 1968, pp. 745-762.
- [10] H. A. Van Der Vorst, "BI-CGSTAB: A fast and smoothly converging variant of BI-CG for the solution of nonsymmetric linear system". SIAM Journal on Scientific and Statistical Computing, Vol. 13, No. 2, 1992, pp. 631-644.
- [11] T. Kunugi, N. Saito, T. Fujita and A. Serizawa, "Direct numerical simulation of pool and forced convective flow boiling phenomena". <u>Proceedings of the twelfth</u>

  <u>International Heat Transfer Conference</u>, Grenoble, France, 2002, August 18-23.
- [12] V.P. Carry, "Liquid Vapor Phase-Change Phenomena: An introduction to the thermophysics of vaporization and condensation process in heat transfer equipment", Taylor & Francis, 1992, pp. 138–140.

- [13] D.B.R. Kenning and Y. Yan, "Pool boiling heat transfer on a thin plate: features revealed by liquid crystal thermography", International Journal of Heat and Mass Transfer, Vol. 39, No. 15, 1996, pp. 3117-3137.
- [14] N.I. Kolev, "To the nucleate boiling theory". Nuclear Engineering and Design, Vol. 239, 2009, pp. 187-192.
- [15] I. Ohnaka, "Introduction to computational analysis of heat transfer and solidification application to the casting processes-", Maruzen, 1985, pp. 202. (in Japanese)
- [16] Y. Ose, Z. Kawara and T. Kunugi, "Numerical simulation of subcooled boiling compared with experimental data and analytical equations". <u>Proceedings of the thirteenth International Topical Meeting on Nuclear Reactor Thermal Hydraulics</u>, Kanazawa, Japan, 2009, September 27-October